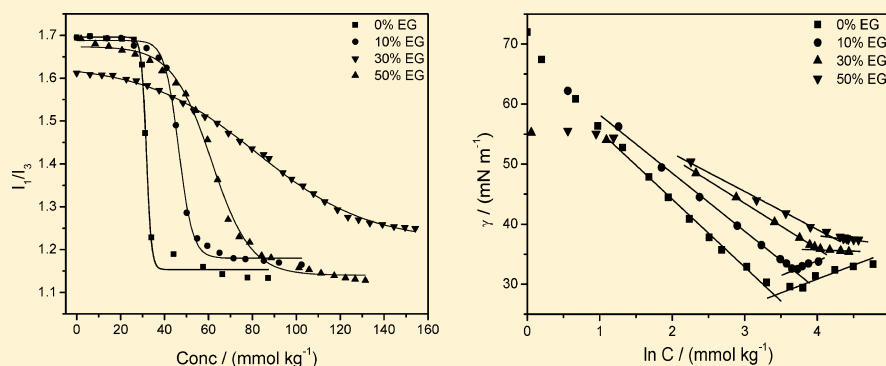


Effect of Ethylene Glycol and Its Derivatives on the Aggregation Behavior of an Ionic Liquid 1-Butyl-3-methyl Imidazolium Octylsulfate in Aqueous Medium

Tejwant Singh,^{*,†} K. Srinivasa Rao, and Arvind Kumar^{*}

Central Salt and Marine Chemicals Research Institute, Council of Scientific & Industrial Research (CSIR), G. B. Marg, Bhavnagar-364002, Gujarat, India

S Supporting Information



ABSTRACT: The effect of ethylene glycol (EG) and its derivatives, ethylene glycol monomethyl ether (EGMME), or ethylene glycol dimethyl ether (EGDME), on the aggregation behavior of a surfactant-like ionic liquid (IL), 1-butyl-3-methyl imidazolium octylsulfate, $[C_4mim][C_8OSO_3]$, in aqueous solutions is investigated using conductivity, surface tension, fluorescence, 1H NMR, and dynamic light scattering (DLS) measurements. Thermodynamic parameters such as Gibbs free energy (ΔG_m°), standard enthalpy (ΔH_m°), and standard entropy (ΔS_m°) of aggregation are determined from the temperature dependence of conductivity. The interfacial properties of IL at the air/water interface in various mixed solvents are evaluated from surface tension measurements. Information about the local microenvironment and size of the aggregates is obtained from steady-state fluorescence using pyrene as a polarity probe and DLS measurements, respectively. 1H NMR data has been employed to get detailed insight into the effect of organic additives on the IL aggregate structure and aggregation number. It has been observed that the addition of organic additives to water decreases the spontaneity of aggregation of IL.

INTRODUCTION

Room temperature ionic liquids (ILs), due to their unique physicochemical properties such as thermal stability, non-flammability, negligible vapor pressure, large liquidus range, wide electrochemical window, etc., are rapidly gaining interest as greener replacements for traditional volatile organic solvents used in chemical processes and have been the focus of many scientific investigations.^{1–12} From recent studies, it has been well established that the inherent amphiphilic character of some ILs leads to the aggregation phenomena in the aqueous, nonaqueous, or even in the ionic liquid media.^{13–32} ILs, owing to the distinct polarizability of head groups, can generate specific self-assembled structures which can act as a novel micellar catalyst, and can show a different or even improved templating behavior for synthesis of nanostructured materials for different applications.^{33–38} Hence, self-assembling behavior of ILs as a novel class of surfactants has aroused much interest. Since mixed solvents are used in many industrial processes, the interest in aggregation properties of ILs in mixed water–organic binary solvents is slowly gaining momentum.^{39–42}

Recently, Wang et al. reported the modulation of the aggregation behavior of a cationic amphiphilic IL, 1-dodecyl-3-methyl imidazolium bromide, by the organic solvents in aqueous media.⁴¹ However, to this date, there are no exhaustive studies examining the influence of organic solvents on the aggregation behavior of ILs. Such studies can be of great importance not only in the field of colloid and interface science but in the development of several chromatographic applications that employ IL aggregates such as micellar liquid chromatography (MLC). Most applications of MLC utilize the hybrid micellar mobile phases which contain surfactants at concentrations above the critical micelle concentration (cmc), forming some sort of ternary systems upon addition of organic solvents.^{43,44} In addition, IL and organic solvent mixtures are becoming more widely studied in various extraction, synthetic, and separation methodologies.^{45–47} Therefore, it is of immense

Received: November 30, 2011

Revised: January 10, 2012

Published: January 12, 2012

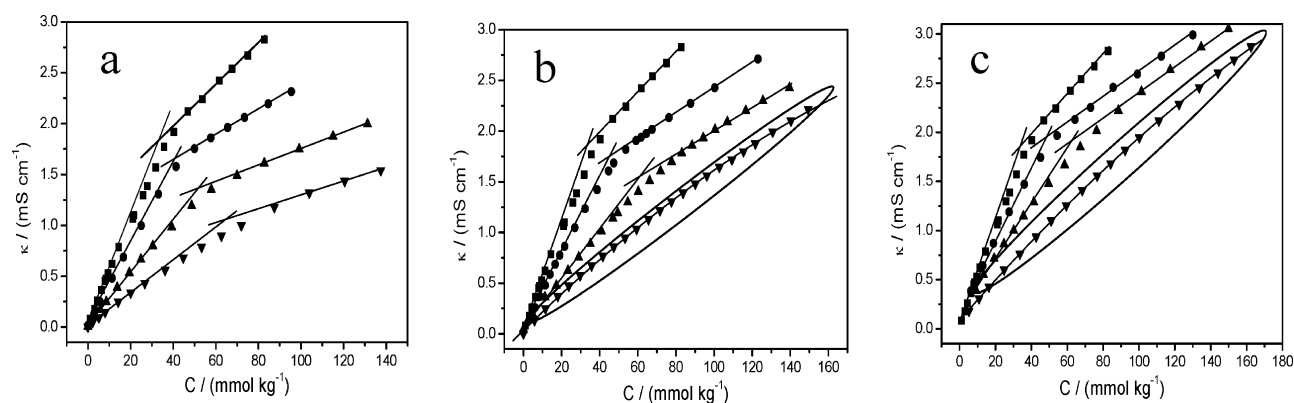


Figure 1. Variation of conductivity as a function of $[C_4mim][C_8OSO_3]$ concentration in water or aqueous-EG/EGMME/EGDME for varying compositions of mixed solvent (■) 0% (w/w); (●) 10% (w/w); (▲) 30% (w/w); (▼) 50% (w/w). The marked area in parts b and c indicates the absence of aggregation.

importance to investigate and understand the effect of organic solvents on the aggregation behavior of ILs. On the other hand, ethylene glycol and its derivatives are a special class of organic additives that are normally used as hydrotropes in conventional colloidal systems.⁴⁸ Therefore, we have initiated a systematic study toward understanding the effect of ethylene glycol and its derivatives on the aggregation behavior of ILs in the aqueous medium.

In the present study, we have investigated the effect of EG, EGMME, and EGDME on the aggregation behavior of a surfactant-like IL, 1-butyl-3-methyl imidazolium octylsulfate, $[C_4mim][C_8OSO_3]$, in aqueous medium. The effect of structural variation in EG by replacing the hydroxyl protons by an ethylene group has been studied and compared. The choice of $[C_4mim][C_8OSO_3]$ for the study was made considering its capability to aggregate strongly in aqueous media.^{14,24} The temperature dependence of conductivity enabled us to explore the thermodynamics of aggregation. The interfacial behavior of $[C_4mim][C_8OSO_3]$ is unique as both cation and anion, being amphiphilic tends to adsorb at the air–water interface. Thus, we used the surface tension measurements to address the interfacial behavior of $[C_4mim][C_8OSO_3]$ in the presence of organic additives. A series of useful parameters were obtained to assess the surface activity of the ILs in these mixed solvents, and are compared to that in pure water. The steady state fluorescence spectroscopy has been used to determine the cac and micropolarity of the IL aggregates. The hydrodynamic radii (R_h) of the aggregates were obtained from dynamic light scattering (DLS) measurements.

NMR, which is a very sensitive technique, has been used before to determine the critical aggregation concentration for classical surfactants⁴⁹ as well as ILs.^{19,20,23,24,27} It has been demonstrated in recent years that on aggregation there are considerable changes in both shielding and relaxation, and it is possible to characterize the effects for a large number of protons in an alkyl chain or aromatic ring.^{19,20,23,24,27,49–57} Therefore, we used the 1H NMR measurements to probe the aggregated structures on a molecular scale. The peculiar upfield/downfield chemical shifts of various IL protons or mixed solvents have been analyzed to unfold the changes in aggregated structures as a consequence of the addition of organic solvents. The aggregation number (N_{agg}) in the preaggregation region and of aggregates was deduced from the application of the law of mass action to 1H NMR chemical shift data.

2. EXPERIMENTAL SECTION

2.1. Materials. 1-Butyl-3-methylimidazolium octylsulfate, $[C_4mim][C_8OSO_3]$, with stated purity higher than 98% mass fraction, was purchased from Solvent Innovation GmbH. Prior to use, the IL was further purified, dried, and degassed under vacuum at 70 °C for 48 h, according to the procedure described in our earlier communication.⁵⁸ The water content in the IL as indicated by Karl Fischer analysis was 0.025%. Ethylene glycol (>99.0 mol %), ethylene glycol monomethyl ether (>99.5 mol %), and ethylene glycol dimethyl ether (>99.0 mol %) were obtained from Loba Chemie, Mumbai, and Merck, respectively. The organic solvents were used after drying over the 0.4 nm molecular sieves and under vacuum at ambient conditions. Aqueous or aqueous-EG/EG derivative mixed solvents of the IL for all measurements were prepared by weight using an analytical balance with a precision of ± 0.0001 g (Denver Instrument APX-200). Aqueous solutions were prepared in degassed Millipore grade water. The concentration of the EG and its derivatives in various binary aqueous solvents were kept as 10, 30, and 50%.

2.2.1. Methods. Conductivity. Ionic conductivities were measured at 288.15, 298.15, and 303.15 K by a digital conductivity meter (Systronics 308) using a cell of unit cell constant (1.0 cm^{-1}). The temperature of the measurement cell was controlled with a Julabo water thermostat within ± 0.1 K. Before the measurements, the conductivity cell was calibrated using the aqueous KCl solutions in the concentration range $0.01\text{--}1.0\text{ mol}\cdot\text{kg}^{-1}$. The measurements were taken in triplicate for each concentration, and only the mean values were taken into consideration. The uncertainty of the measurements was less than 0.3%.

2.2.2. Surface Tension Measurements. Surface tension measurements were carried out at 298.15 K using a DataPhysics DCAT II automated tensiometer employing the Wilhelmy plate method. IL was added into the water or water-EG/EG derivative mixed solvent by weight and stirred for 3–4 min for complete solubilization. Prior to measurements, the resultant solutions were kept for at least 10 min for equilibration. The data was collected in duplicate and was found to be accurate within $\pm 0.1\text{ mN}\cdot\text{m}^{-1}$. The temperature of the measurement cell was controlled with a Julabo water thermostat within ± 0.1 K.

2.2.3. Fluorescence Measurements. Steady state fluorescence measurements were performed using a Fluorolog (Horiba Jobin Yvon) spectrometer using a quartz cuvette of

Table 1. Experimentally Determined cac from Various Techniques, Degree of Counterion Dissociation (α), Standard Free Energy of Aggregation (ΔG_m°), Standard Enthalpy of Aggregation (ΔH_m°), Standard Entropy of Aggregation (ΔS_m°), and Relative Intensity of Vibronic Bands (I_1/I_3) of Pyrene Fluorescence at 298.15 K

	cac (mmol kg ⁻¹)				α	ΔG_m° ^a	ΔH_m° ^a	ΔS_m° ^a	I_1/I_3
	cond	flr	ST	¹ H NMR					
water	36.0 ^b	31.0	30.5	37.0 ^b	0.39	−30.1	−11.0	0.064	1.15
EG 10%	39.2	45.0	39.4	32.3	0.30	−30.6	−3.1	0.092	1.18
EG 30%	49.3	59.1	56.2	52.3	0.29	−30.7	−4.4	0.088	1.19
EG 50%	63.0	74.5	62.0		0.34	−28.8	−10.5	0.055	1.25
EGMME 10%	45.0	46.8	38.2	47.0	0.33	−29.4	−5.0	0.082	1.12
EGMME 30%	58.0	64.6	64.7	68.5	0.48	−26.7	−8.8	0.057	1.26
EGDME 10%	41.0	53.8	41.2	49.5	0.36	−30.4	−6.4	0.080	1.02
EGDME 30%	59.0	77.0	49.15	60.6	0.46	−27.0	−10.7	0.055	1.33

^a ΔG_m° , ΔH_m° , and ΔS_m° are expressed in kJ mol⁻¹. ^bData used from ref 24.

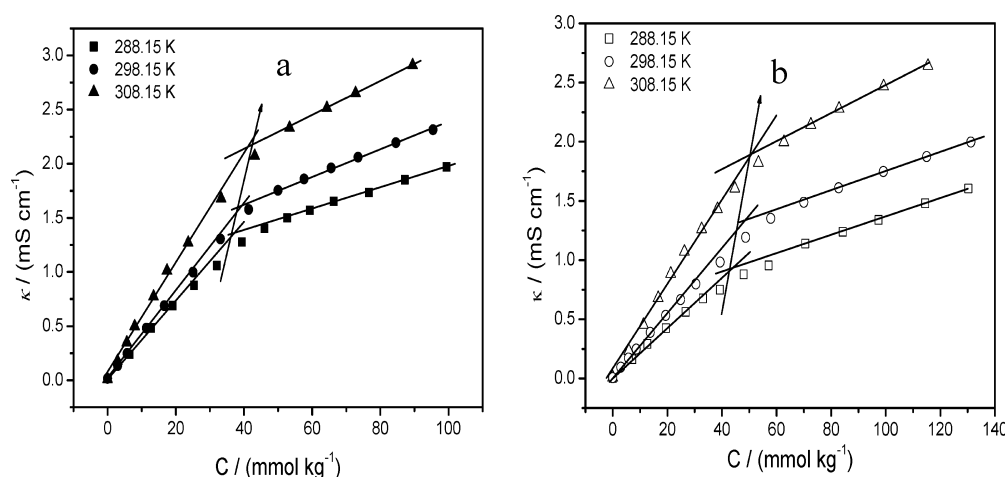


Figure 2. Variation of conductivity as a function of $[C_4mim][C_8OSO_3]$ concentration in aqueous-EG mixed solvent: (a) 10% (w/w) EG; (b) 30% (w/w) EG at different temperatures. The arrow depicts the increase in cac.

path length 1 cm. Pyrene was used as the polarity probe, as the ratio (I_1/I_3) of its first vibronic peak (373 nm, I_1) to third vibronic peak (384 nm, I_3) is very sensitive to the polarity of the surroundings. The emission spectra of pyrene were recorded in the wavelength range 350–500 nm at an excitation wavelength of 334 nm using the excitation and emission slit widths of 1 nm. The concentration of pyrene used was 2 μ M. The fluorescence spectra were corrected for the instrumental response.

2.2.4. Dynamic Light Scattering. The dynamic light scattering measurements (DLS) were performed at 298.15 K on a light scattering apparatus described elsewhere.⁵⁹ Appropriate amounts of ILs were added by weight to the water or water-EG/EG derivative binary solvent (2 mL) taken in a cylindrical quartz cuvette for DLS measurements. The temperature for the measurements was controlled with an accuracy of ± 0.1 K.

2.2.5. NMR Measurements. The ¹H NMR spectra for the various IL solutions were recorded using a Bruker 500 MHz spectrometer. The proton chemical shifts were referenced with respect to an external standard TMS ($\delta = 0.000$ ppm) in C_6D_6 (deuterated benzene). The chemical shifts of the peaks of interest were determined using a peak pick facility.

3. RESULTS AND DISCUSSION

3.1.1. Conductivity Measurements. Critical Aggregation Concentration and Degree of Dissociation. The

measurements of conductivity in various aqueous or aqueous-EG/EG derivative mixed solvents as a function of $[C_4mim][C_8OSO_3]$ concentration at 298.15 K are shown in Figure 1. Distinct break points in the conductivity vs concentration profiles of the IL solutions were observed as the critical aggregation concentration (cac) of ILs and are given in Table 1. At the higher concentration of organic solvents, the break point in the conductivity profile is not clear; hence, the method given by Carpena et al. was used to determine the cac values accurately.⁶⁰ The cac of the $[C_4mim][C_8OSO_3]$ increased with the increase in content of organic additives. The cac increased least in the case of EG as compared to EGMME or EGDME for the same amount of organic solvent added. This may be due to the resemblance of EG with water in some properties such as high cohesive energy density and capability of hydrogen bonding, and, therefore, did not affect the aggregation to some extent. For the same amount of EG/EG derivatives added, the aggregation has been found to diminish in the order EG < EGMME < EGDME. This may be due to the increased solvophobic effect of solvent as a consequence of replacement of the hydroxyl proton of EG by a methylene group. With a still higher concentration of EGMME or EGDME [50% (w/w)], no distinct break point in the conductivity profiles of IL solutions was observed, indicating the absence of spontaneous aggregation of $[C_4mim][C_8OSO_3]$ (marked areas in Figure 1). The degree of counterion dissociation, α , which was calculated from the ratio of the slope (S_2/S_1) of linear

fragments of conductivity profiles of postaggregation (S_2) to preaggregation (S_1) region, is given in Table 1. α increases with the increase in either the amount of EG/EG derivative or EG substitution and follows the order $EG < EGMME < EGDME$, indicating the decreased counterion binding in the Stern layer of the aggregates.

As the conductivity results showed the absence of spontaneous aggregation of $[C_4mim][C_8OSO_3]$ in 50% (w/w) EGMME or EGDME, the temperature dependent studies were done for solvent composition up to 30% (w/w). The temperature dependence of conductivity for the system having 10 and 30% (w/w) of EG is shown in Figure 2a and b, respectively. As can be seen from Figure 2, the cac increases with an increase in temperature for both concentrations of EG. Similar results have been observed for other systems having EG derivatives. For the same amount of EG/EG derivative, the temperature dependency of cac followed the order $H_2O < EG < EGMME < EGDME$. This indicates the better solvophobic effect of EGDME as compared to EG or EGMME for $[C_4mim][C_8OSO_3]$ in water.

3.1.2. Thermodynamics of Aggregation. The temperature dependence of conductivity was employed to elucidate the thermodynamics of aggregation of $[C_4mim][C_8OSO_3]$ in various mixed solvents. The standard Gibbs free energy of aggregation, ΔG_m° , of $[C_4mim][C_8OSO_3]$ in various mixed solvents was derived according to the pseudo phase model of micellization⁶¹

$$\Delta G_m^\circ = (2 - \alpha)RT \ln x_{cac} \quad (1)$$

where x_{cac} is the cac expressed on a mole fraction scale. The estimated values of ΔG_m° in various solvents are reported in Table 1. For the various solvents, ΔG_m° behaves similar to α . With the increase in the amount of organic solvent or EG derivatization, ΔG_m° becomes less negative and follows the order $EG < EGMME < EGDME$. This indicates the decrease in spontaneity of aggregation with the increase in amount of EG/EG derivatives or EG derivatization. ΔG_m° in the water-EG mixed solvent system is very much close to that observed in water as compared to other mixed solvents. EG is a well-known structure-breaking solute for water;⁶² such solutes decreased the hydrophobicity of the surfactants and disfavor micellization.⁶³ The change in ΔG_m° and other aggregation parameters such as cac and α can be better explained using the solvophobic effect which can be approximately accounted for by considering the changes in the bulk phase cohesive energy density, expressed by the Gordon parameter. The above observations can be explained by considering the following contributions to ΔG_m° :⁶⁴ (i) the surfactant tail transfer Gibbs energy, $\Delta G_{m,trans}^\circ$, accounts for the energy change accompanying the transfer of the surfactant tail from the bulk phase into the aggregate interior; (ii) the interfacial Gibbs energy, $\Delta G_{m,int}^\circ$, takes into account the formation of an interface between the aggregate core and the bulk phase; (iii) the electrostatic Gibbs energy, $\Delta G_{m,ele}^\circ$, considers the electrostatic repulsions between the surfactant head groups at the aggregate surface; (iv) the deformation Gibbs energy, $\Delta G_{m,deg}^\circ$, takes into account the change in tail conformation inside the aggregate as compared to the pure state; (v) the steric Gibbs energy, $\Delta G_{m,steroc}^\circ$, considers the steric repulsions between head groups of surfactants at the aggregate surface. $\Delta G_{m,trans}^\circ$, $\Delta G_{m,int}^\circ$, and $\Delta G_{m,ele}^\circ$ are the only solvent dependent contributions. Therefore, one can consider that the experimental changes in ΔG_m° upon addition of EG or its derivatives resulted from the changes in one or more of

these contributions. Water–glycol mixtures are better solvents for surfactant molecules than pure water.⁶⁵ This disfavors the aggregation process, as the hydrophobic tail transfer from the bulk phase into the aggregates is less favorable and resulted in an increase in $\Delta G_{m,trans}^\circ$ (less negative). Therefore, the increase in the content of EG or its derivatives increases the cac, and hence increases ΔG_m° . One can neglect the dependence of ΔG_m° on $\Delta G_{m,int}^\circ$ due to its very small contribution. $\Delta G_{m,ele}^\circ$, which depends on bulk phase permittivity, governs the electrostatic repulsions between the head groups. As the increase in concentration of EG/EG derivatives or derivatization of EG diminishes bulk phase permittivity, the headgroup repulsions should increase.^{64,65} To overcome the headgroup repulsions, α should decrease. However, the observed trend is reverse. A similar observation has been reported for the micellization of conventional surfactants in mixed solvent media having water and EG or its derivatives.⁶⁶ This result can be further investigated by gaining information about the effects of EG or its derivatives addition on the minimum surface area per headgroup at the air–solution interface (discussed in section 3.2). The addition of organic solvent increases the cac substantially, leading to an increase in the ionic concentration in the bulk phase which consequently causes screening of the headgroup charges. The observed increment in α provoked by EG or its derivatives addition points out that the reduction in the electrostatic repulsions caused by the ionic concentration increment compensates the increment in $\Delta G_{m,ele}^\circ$ originated by the decrease in the bulk phase permittivity.

The dependence of ΔG_m° on the concentration of EG or its derivatives can be qualitatively explained by the increment in the cac and α . The quantification of these effects can be done by considering the changes produced in the bulk phase cohesive energy density as described by the Gordon parameter (G),⁶⁷ which is expressed as $G = \gamma/V_m^{1/3}$, where γ is the air/solvent surface tension and V_m the molar volume of the solvent. The Gordon parameter characterizes the ability of a solvent to bring about the self-association of conventional amphiphiles.⁶⁸ Figure 3 shows the variation of ΔG_m° with G . ΔG_m° decreases

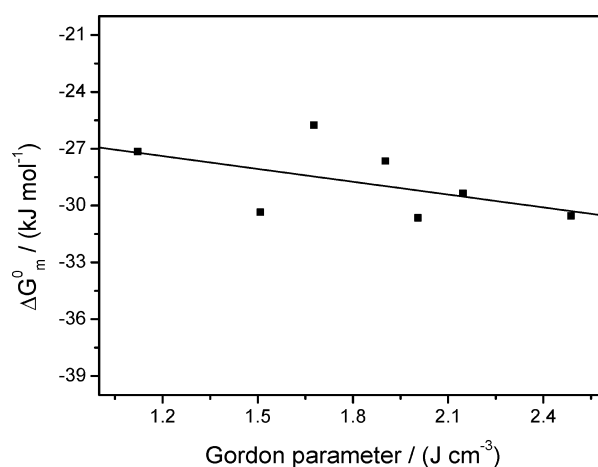


Figure 3. Variation of standard free energy of aggregation (ΔG_m°) with Gordon parameter (G) at 298.15 K. The line is just a guide to the eye.

with an increase in G , indicating that the changes in ΔG_m° of $[C_4mim][C_8OSO_3]$ are caused by addition of EG/its derivatives and can be approximately estimated by considering the modifications produced in G of the bulk phase by the

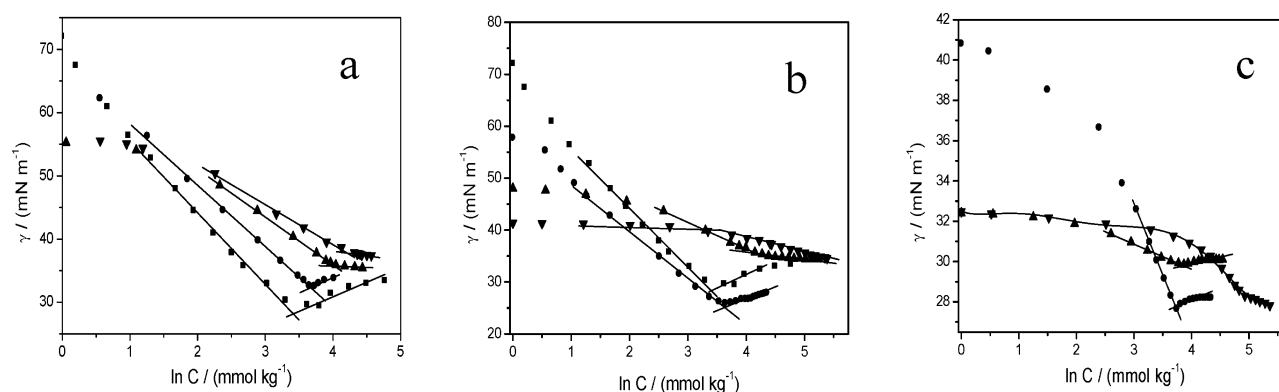


Figure 4. Variation of surface tension as a function of $[C_4mim][C_8OSO_3]$ concentration in aqueous or aqueous-EG/its derivatives mixtures at 298.15 K: (a) aqueous-EG; (b) aqueous-EGMME; (c) aqueous-EGDME for varying compositions of mixed solvents: (■) 0% (w/w); (●) 10% (w/w); (▲) 30% (w/w); (▼) 50% (w/w).

Table 2. Experimentally Determined Surface Tension at cac (γ_{cac}) and Calculated Surface Pressure (π_{cmc}), Gibbs' Surface Excess (Γ_{max}), Area of Exclusion per Monomer (A_{min}), and Standard Free Energy of Adsorption (ΔG_{ad}°), Hydrodynamic Radii (R_h), and Aggregation Number (N_{agg}) at 298.15 K^a

solvent	γ_{cac}	π_{cmc}	$\Gamma_{max} \times 10^6$	A_{min}	ΔG_{ad}°	R_h (nm)	N_{agg} (NMR)
water	29.6	42.4	2.18	0.76	−49.5	1.4	27 ^b
EG 10%	32.5	34.7	1.95	0.85	−48.4	2.2	22
EG 30%	35.9	20.5	1.53	1.08	−44.1	2.0	20
EG 50%	37.3	19.1	0.87	1.90	−48.9		
EGMME 10%	25.8	31.9	1.84	0.90	−46.7	2.3	20
EGMME 30%	34.9	13.4	1.03	1.62	−38.7	1.4	16
EGDME 10%	27.6	13.0	1.43	1.16	−40.6	2.3	18
EGDME 30%	29.9	1.1	0.26	6.33	−31.2	1.9	17

^a ΔG_{ad}° is expressed in kJ mol^{−1}, and γ_{cac} , π_{cmc} , Γ_{max} and A_{min} are expressed in mN m^{−1}, mN m^{−1}, mol m^{−2}, and nm² molecule^{−1}, respectively. ^bData used from ref 24.

addition of EG/its derivatives. Similar results have also been reported for conventional ionic surfactants.^{66,68}

The standard enthalpy of aggregation, ΔH_m° , can be derived from the ΔG_m° values as a function of temperature by applying the Gibbs–Helmholtz equation:

$$\left[\frac{\partial(\Delta G_m^\circ/T)}{\partial(1/T)} \right] = \Delta H_m^\circ \quad (2)$$

The slopes of variation of $\Delta G_m^\circ/T$ as a function of $1/T$ give ΔH_m° at respective temperatures. The standard entropy of aggregation, ΔS_m° , was obtained by the use of the following relation:

$$\Delta S_m^\circ = \Delta H_m^\circ - \Delta G_m^\circ/T \quad (3)$$

The thermodynamic parameters for the aggregation of $[C_4mim][C_8OSO_3]$ in water or water-EG/EG derivative mixed solvents are provided in Table S1 (Supporting Information). The values obtained at 298.15 K are also reported in Table 1. We have observed some common thermodynamic characteristic features in all binary solvent mixtures. When compared to pure water, ΔG_m° did not change much for the solutions with 10 wt % of the organic solvents, whereas it reduced considerably with the addition of 30 wt % of organic solvent. ΔH_m° decreased with the increase in temperature and remained negative in the studied temperature range, indicating the aggregation process as an exothermic one at these temperatures. For the same amount of added EG/its derivatives, ΔH_m° (negative) varies in the order EG < EGMME < EGDME, indicating the increase in enthalpy control over the

aggregation with EG derivatization. A small decrease in $-T\Delta S_m^\circ$ has been observed while going from EG to EGDME, while it decreased to a significant extent with the increase in concentration of organic additives. The observation about ΔH_m° and $-T\Delta S_m^\circ$ indicates that, at low organic solvent concentration, ΔH_m° governs the change in ΔG_m° , while $-T\Delta S_m^\circ$ dictates the change at higher organic solvent concentration.

3.2. Surface Tension Measurements. The concentration profiles of surface tension in the various water-EG/EG derivative mixed solvents at 298.15 K are presented in Figure 4. The cac's obtained from surface tension measurements are reported in Table 1, and other derived parameters are given in Table 2. The cac obtained from surface tension measurements is found in close agreement with that observed from conductivity measurements. As can be seen from Figure 4b and c, similar to conductivity results, no onset of aggregation in the mixed solvent having 50% (w/w) EGMME or EGDME is observed, as indicated by the absence of a surface tension plateau after a certain minimum value. The value of surface tension at cac (γ_{cac}) was found to be increased with an increase in EG/its derivatives concentration. The effectiveness of surface tension reduction (π) also called surface pressure at the saturated air/solution interface is calculated as

$$\pi_{cac} = \gamma_0 - \gamma_{cac} \quad (4)$$

where γ_0 and γ_{cac} are the surface tension of solvent and surface tension at the cac. This parameter indicates the maximum reduction of surface tension caused by the dissolution of surfactant molecules and hence becomes a measure for the effectiveness of the surfactant to lower the surface tension of

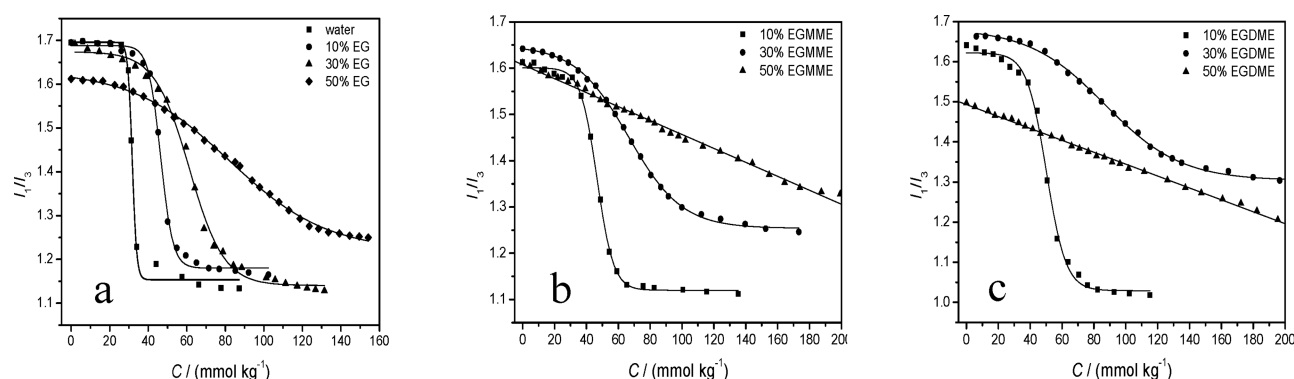


Figure 5. Variation of I_1/I_3 of pyrene as a function of $[\text{C}_4\text{mim}][\text{C}_8\text{OSO}_3]$ concentration in various aqueous or aqueous-EG/EG derivative mixtures at 298.15 K: (a) aqueous or aqueous-EG; (b) aqueous-EGMME; (c) aqueous-EGDME for varying compositions of mixed solvents.

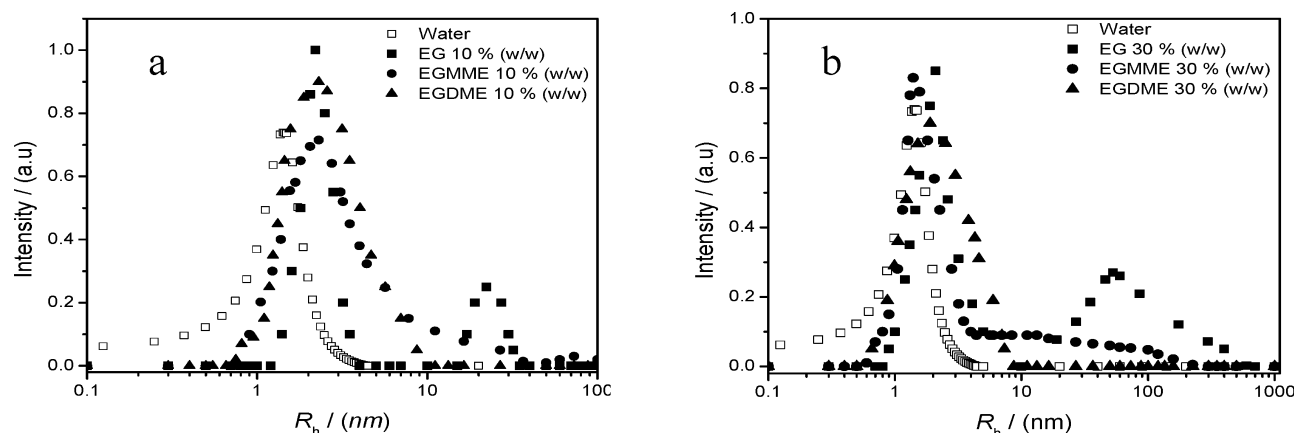


Figure 6. Variation of the size distribution of $[\text{C}_4\text{mim}][\text{C}_8\text{SO}_4]$ aggregates in various aqueous-EG/its derivatives mixtures as a function of the composition of binary solvent from DLS measurements at 298.15 K.

the solvent. π_{cac} was found to be higher in water as compared to water-EG/EG derivative mixed solvents and followed the order $\text{H}_2\text{O} > \text{EG} > \text{EGMME} > \text{EGDME}$ at each organic solvent concentration. Moreover, the increase in concentration of EG/its derivatives decreases the π_{cac} , indicating the deterioration of surface activity of $[\text{C}_4\text{mim}][\text{C}_8\text{OSO}_3]$.

By applying the Gibbs adsorption isotherm to the tensiometric profiles in the concentration range below and close to the cac, the maximum surface excess concentration (saturation adsorption), Γ_{max} , and the minimum area occupied by a single IL molecule at the air–solution interface, A_{min} , can be estimated.⁶⁹ The Gibbs equation for monovalent ionic surfactants (valid for the ILs studied) is given as

$$\Gamma_{\text{max}} = -\frac{1}{nRT} \lim_{C \rightarrow 0} \left(\frac{\partial \gamma}{\partial \ln C} \right)_T \quad (5)$$

where R is the gas constant, T is the absolute temperature, n is 2 for IL (as the IL generates two ions upon dissociation in water), and C is the IL concentration in bulk solution. From the obtained Γ_{max} , A_{min} can be calculated using the equation

$$A_{\text{min}} = \frac{1}{N_A \Gamma_{\text{max}}} \quad (6)$$

where N_A is the Avogadro number. The observed values of Γ_{max} and A_{min} are reported in Table 2. Γ_{max} decreases and A_{min} increases with an increase in content of EG/EG derivative, and for the same organic solvent concentration, it follows the order $\text{H}_2\text{O} > \text{EG} > \text{EGMME} > \text{EGDME}$. This indicates that the

packing of IL molecules at the interface decreases with an increase in EG/its derivatives as well as with EG derivatization. A_{min} followed the reverse trend to that of Γ_{max} , as it increases with an increase in concentration of EG/its derivatives and with EG derivatization. The presence of EG/its derivatives results in the bulk phase becoming a better solvent for the IL molecules than pure water, leading to easy solubilization of IL molecules and thereby decreasing their adsorption efficiency at the interface.

3.3. Fluorescence Measurements. Figure 5 shows the variation of I_1/I_3 with IL concentration in various mixed solvents. The ratio I_1/I_3 remains constant up to a certain concentration and then decreases rapidly, which again attains an almost constant value with further increase in IL concentration. The cac's derived from the midpoint of transition in I_1/I_3 are given in Table 1 and are in good agreement with the cac's observed from other methods with the exception of EGDME (30%) where the cac observed from fluorescence measurements is on the higher side. No aggregation of IL has been observed in the mixed solvent having 50% (w/w) EGMME or EGDME as observed from the almost linear variation of I_1/I_3 with IL concentration. Therefore, we restricted our further studies (DLS and ^1H NMR measurements) to the 10 and 30% (w/w) water-EG/EG derivative mixed solvents. These results are similar to those observed from conductivity and surface tension measurements. In the mixed solvents having low organic solvent content (10% w/w), before aggregation, a sharp decrease in I_1/I_3 has been

Scheme 1. Molecular Structure and Molecular Formulae of IL and Various Organic Solvents

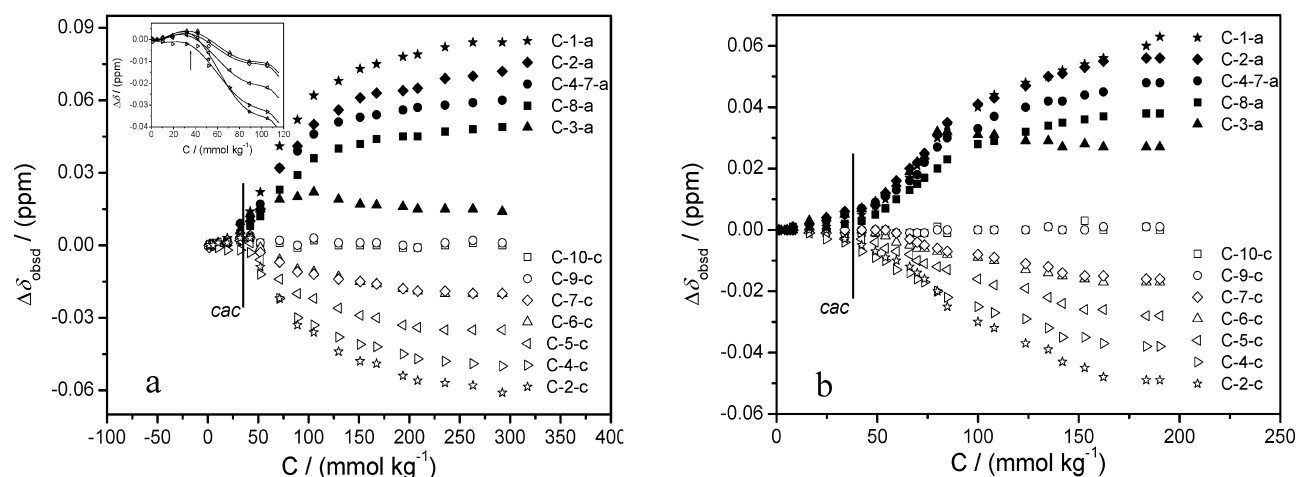
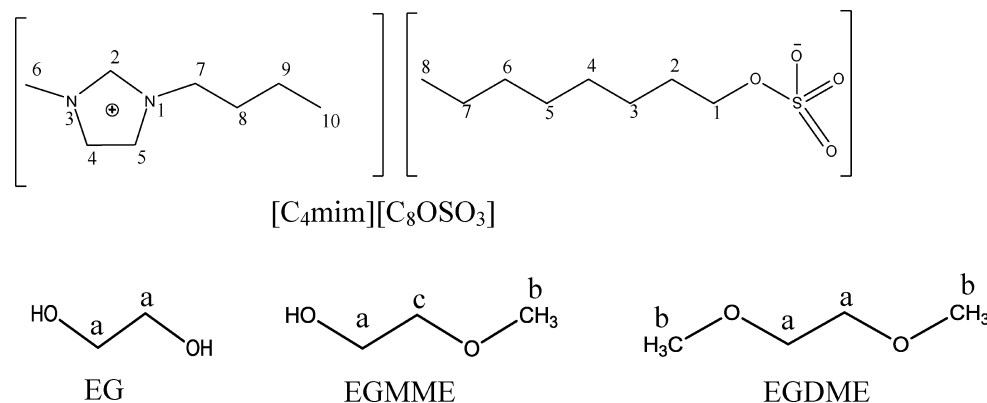


Figure 7. The variation of $\Delta\delta_{\text{obsd}}$ ($\delta_{\text{obsd}} - \delta_{\text{mon}}$) for various protons of anion and cation of [C₄mim][C₈OSO₃] as a function of IL concentration in binary mixtures of water and EG at different EG contents: (a) EG 10% (w/w); (b) EG 30% (w/w). The proton numbering is according to Scheme 1. (a and c) correspond to the anion and cation, respectively.

observed, whereas, at higher content of organic solvent, the I_1/I_3 changes slowly. For the same concentration of EG/its derivatives, the slope change of I_1/I_3 upon aggregation decreases with an increase in EG derivatization in the order $\text{H}_2\text{O} \approx \text{EG} < \text{EGMME} < \text{EGDME}$. This indicates that both the increasing content of organic solvent and its derivatization makes the aggregation less spontaneous, supporting our thermodynamic findings.

The vibronic structure of the fluorescence spectrum of monomeric pyrene is known to be sensitive to the local polarity (cybotactic region), as sensed by pyrene, and is indicated by the change in ratio I_1 and I_3 of pyrene (Supporting Information, Figure S1). The ratio I_1/I_3 of solubilized pyrene increases on going from nonpolar to polar solvents.⁷⁰ The value of I_1/I_3 upon completion of aggregation in various binary solvents is given in Table 1. The I_1/I_3 goes on increasing both with the increase in content of EG/its derivatives as well as EG derivatization, indicating the increase in polarity of pyrene's cybotactic region which may be due to incorporation of organic solvent molecules in the Stern layer of aggregates or in the interior of aggregates forming loose aggregates. The I_1/I_3 in EG (10 or 30% w/w) is very close to that observed in water, indicating the aqueous-EG mixed solvents in low concentrations are as good as water for aggregation of [C₄mim]-[C₈OSO₃].

3.4. Dynamic Light Scattering. Variation in the hydrodynamic radii (R_h) of the aggregate as a function of the nature of the organic solvent and its content in aqueous binary solvents has been investigated through DLS measurements. The CONTIN plots, corresponding to the radii distribution functions of IL aggregates in aqueous or various aqueous-EG/EG derivative mixed solvents, are shown in Figure 6, and the corresponding R_h is given in Table 2. The R_h of aggregates formed in mixed solvents was found to be higher than that in water,²⁴ which, however, decreased with an increase in content of EG/its derivatives. For the same amount of organic additive, R_h varies in the order $\text{H}_2\text{O} < \text{EG} < \text{EGMME} < \text{EGDME}$. The increased size of the aggregates at lower organic additive content in the solution may be due to (i) the increase in aggregation number or (ii) the swelling (loosening) of aggregates by the incorporation of solvent molecules into the aggregates. The swelling of the aggregates was also observed from the fluorescence measurements. At a higher concentration of organic additive (30 wt %), the decrease in size may be due to increased solubilization of IL by the organic solvent.

3.5.1. ¹H NMR Measurements. *Protons of Cation and Anion.* The nature of self-assembled structures of [C₄mim]-[C₈OSO₃] in various aqueous-EG/its derivatives mixed solvents was investigated using ¹H NMR spectroscopy. In contrast to the other techniques, ¹H NMR is a direct molecular approach that uses native molecular probes and has been found

very useful in elucidating the structures at the molecular level. The chemical shifts of IL protons as well as of solvents were resolved in ^1H NMR spectra. The ^1H NMR chemical shifts (δ_{obsd}) of IL protons, particularly the alkyl chain protons, are very sensitive to conformational and environmental changes occurring during the process of aggregation; therefore, the δ_{obsd} value as a function of concentration of IL in various mixed solvents for each and every proton of cation and anion was examined carefully. The proton numbering of IL is according to Scheme 1. $\Delta\delta_{\text{obsd}}(\delta_{\text{obsd}} - \delta_{\text{mon}})$ as a function of IL concentration for various protons of anion and cation in aqueous mixtures of EG (10 and 30% w/w) showed pronounced changes, and are visualized in Figure 7. Here, δ_{mon} corresponds to the chemical shift of different protons of IL monomers derived by the extrapolation of δ_{obsd} to zero IL concentration. For the mixtures with EG derivatives, $\Delta\delta_{\text{obsd}}$ is depicted in Figures S2–S5 (Supporting Information). A sudden change in $\Delta\delta_{\text{obsd}}$ for various protons of anion has been observed at around cac, owing to the onset of aggregation at the cac. The cac observed for the investigated systems from ^1H NMR measurements is provided in Table 1. The observed cac has been found well in agreement with those obtained from other techniques. The protons of the alkyl chain in the vicinity of polar head groups remain under the influence of electrostatic and steric interactions and do not clearly reflect the conformational changes during the aggregation process, whereas the protons toward the end of the alkyl chain are sensitive to conformational changes arising from various reasons such as packing density and van der Waals or hydrophobic interactions.⁷¹ As can be seen from Figure 7, an upfield shift of different extent has been observed for various protons of the octyl chain of the anion. Since an upfield shift can be related to an increasing importance of van der Waals interactions and gauche conformation, it can be inferred that the aggregation is accompanied by a partial changeover from trans to gauche conformations in the alkyl chain.⁷² The magnitude of $\Delta\delta_{\text{obsd}}$ is maximum for C-1-a and follows the order C-1-a > C-2-a > C-4-7-a > C-8-a > C-3-a. The C-1-a and C-2-a lie in the vicinity of the polar headgroup where the change in electrostatic and steric interaction due to solubilization of organic additive leads to such large change in chemical shift. It was observed that the proton at C-3-a was least sensitive toward aggregation; however, initially, it shows an upfield and then downfield shift at higher concentrations, indicating some conformational changes upon aggregation. When different organic additives are compared, for the same concentration of EG/its derivatives, it was observed that, for various protons of anion, $\Delta\delta_{\text{obsd}}$ varies in the order $\text{H}_2\text{O} > \text{EG} > \text{EGMME} > \text{EGDME}$, indicating the decrease in spontaneity of aggregation with the derivatization of EG. The aggregation process was also found to diminish with an increase in the content of organic additive in the solution.

As can be seen from Figure 7, the protons of imidazolium cation show a downfield shift with increase in IL concentration. In the case of EG (10%), the protons of the cation except C-9-c and C-10-c initially show an upfield shift up to the cac and then shift downfield at higher IL concentrations. The initial upfield shift can be due to aromatic ring induced shielding of protons of the cation near the imidazolium ring or due to solvent effects. The downfield shift for imidazolium protons can be correlated with decreased hydrophilic character of the cation as a consequence of adsorption as counterions in the Stern layer of the aggregates. Various protons of the cation show different

extents of downfield shift in various mixed solvents and followed the order C-2-c > C-4-c > C-5-c > C-6-c \approx C-7-c > C-9-c \approx C-10-c. The protons present at the terminal end of butyl chain (C-10-c and C-9-c) showed no change in $\Delta\delta_{\text{obsd}}$, indicating a negligible change in environment of these protons upon aggregation. These protons seem to remain in the Stern layer of aggregates interacting with the solvent molecules similar to that in bulk. As the protons at C-6-c and C-7-c are close to the imidazolium ring, the change in direction of ring current of the imidazolium ring as a consequence of aggregation resulted in a change in $\Delta\delta_{\text{obsd}}$. The imidazolium ring protons C-2-c, C-4-c, and C-5-c showed maximum change in $\Delta\delta_{\text{obsd}}$, which may be due to the combined effect of ring currents as well as hydrogen bonding interactions with the polar anionic headgroup. The hydrogen bonding interactions between ring protons and polar head groups lead to deshielding of ring protons, thus resulting in higher downfield shift, whereas such interactions are absent for other protons. The EG derivatization or increase in the content of organic additive in the mixed solvent affects the $\Delta\delta_{\text{obsd}}$ of cationic protons in a similar fashion as that for anionic protons.

3.5.2. Protons of the Solvent Molecules. The molecular structures of the EG or its additives used in this study are given in Scheme 1. Figure 8 shows the variation of $\Delta\delta_{\text{obsd}}(\delta_{\text{obsd}} -$

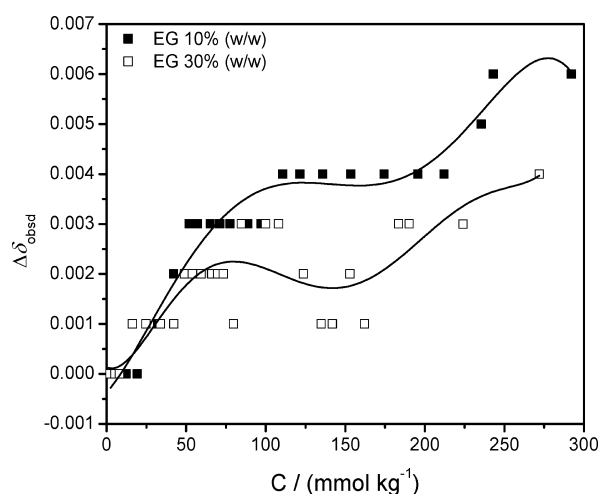


Figure 8. The variation of $\Delta\delta_{\text{obsd}} (\delta_{\text{obsd}} - \delta_{\text{initial}})$ for EG protons (H-a of EG) in water-EG binary solvents as a function of IL concentration at different EG contents: (■) 10% (w/w); (□) 30% (w/w) EG. The lines are just guides to the eye.

$\delta_{\text{initial}})$ for the different protons of EG as a function of IL concentration, and the variation in $\Delta\delta_{\text{obsd}}$ for the protons of EG derivatives is shown Figures S6 and S7 (Supporting Information). As can be seen from Figure 8, the protons of EG do not show any significant change in $\Delta\delta_{\text{obsd}}$, indicating the absence of electronic environment change for these protons upon aggregation at both the EG concentrations. The hydroxyl protons of both EG/EGMME and H_2O resonate at the same position, and therefore, we could not resolve them in the ^1H NMR spectra. As can be seen from Figure S6 (Supporting Information), the protons at positions c-a, c-b, and c-c of EGMME showed an upfield shift at lower EGMME content (10% w/w) with an increase in IL concentration, and their magnitude varies in the order H-a > H-b > H-c. At higher EGMME content (30 wt %), c-a, c-b, and c-c of EGMME showed a significant downfield shift up to the cac which then

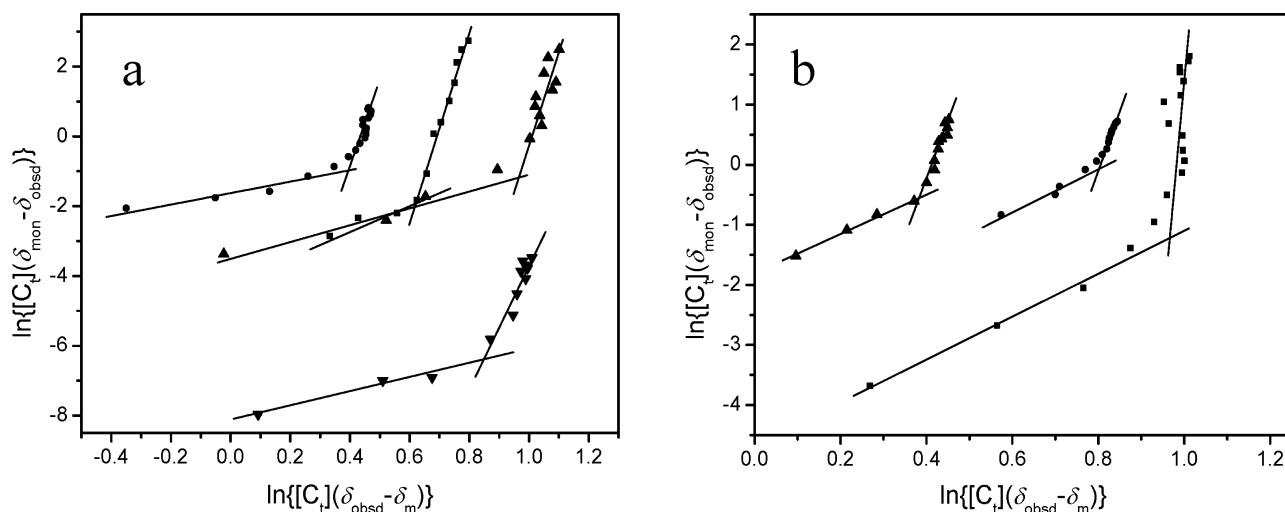


Figure 9. The ^1H NMR data plotted according to eq 12 for $[\text{C}_4\text{mim}][\text{C}_8\text{OSO}_3]$ in water and various aqueous mixtures of EG/its derivatives: (a) 10% (w/w); (b) 30% (w/w). [(▼) water; (■) EG; (●) EGMME; (▲) EGDME].

shifts upfield at higher IL concentrations. The upfield shift after the cac is indicative of some hydrogen bonding interactions between EGMME and the polar headgroup of the anion and cation upon aggregation in the Stern layer. $\Delta\delta_{\text{obsd}}$ for the different protons of EGMME (30%) followed the order H-b > H-c > H-a. In the case of EGDME (Figure S7, Supporting Information), all the protons showed an upfield shift at both EGDME concentrations. When all three systems are compared, the results can be summarized as follows: (i) with an increase in the content of EG/its derivatives, the magnitude of $\Delta\delta_{\text{obsd}}$ diminishes with the exception of EGDME for which it increases; (ii) for the same amount of EG/its derivatives, $\Delta\delta_{\text{obsd}}$ varies in the order EG < EGMME < EGDME, indicating their increasing solvating ability for the IL and thus disfavoring aggregation process.

3.5.3. Aggregation Number. Since the solvent effects are small for alkyl groups in the aggregates, we employed the mass action law to the dependence of δ_{obsd} of protons of the terminal methyl group of the octyl chain on the IL concentration for the determination of aggregation number (N_{agg}). The mass action law for the free IL–aggregate equilibrium



gives

$$K = [A_n]/[A]^n \quad (8)$$

where n is the aggregation number and K the equilibrium constant. Thus, the chemical shift can be written as^{73,74}

$$\delta_{\text{obsd}} = \frac{C_m}{C_t} \delta_m \quad (9)$$

where C_m and C_t are the concentration of aggregated IL and the total concentration, respectively, δ_{obsd} is the observed chemical shift, and δ_m the shift of aggregated IL determined by extrapolation to zero IL concentration. It is possible to express the concentration of monomer as

$$[A] = C_t \frac{\delta_m - \delta_{\text{obsd}}}{\delta_m} \quad (10)$$

and the aggregate concentration as

$$n[A_n] = C_t \frac{\delta_{\text{obsd}}}{\delta_m} \quad (11)$$

Then, the expression for K may be written as

$$\begin{aligned} \log\{[C_t](\delta_{\text{mon}} - \delta_{\text{obs}})\} \\ = n \log\{[C_t](\delta_{\text{obsd}} - \delta_m)\} + \log(nK) + (1 - n) \\ \log(\delta_{\text{mon}} - \delta_m) \end{aligned} \quad (12)$$

Plots of $\log\{[C_t](\delta_{\text{mon}} - \delta_{\text{obs}})\}$ against $\log\{[C_t](\delta_{\text{obsd}} - \delta_m)\}$ yield the aggregation number. Figure 9a and b shows chemical shift data for the terminal alkyl chain proton of the anion plotted according to eq 12 in various aqueous-EG/its derivatives mixed solvents at 10 and 30% organic additive content, respectively. The obtained N_{agg} are given in Table 2 and are compared with that obtained in water. The N_{agg} decreased with the increase in content of EG/its derivatives, and for the same amount of EG/its derivatives, it follows the order $\text{H}_2\text{O} > \text{EG} > \text{EGMME} > \text{EGDME}$. From the slope obtained before the cac using eq 12, smaller preaggregation aggregates comprising of ~ 2 – 3 IL monomers were observed. The preaggregation was found to increase with an increase in EG/its derivatives content.

CONCLUSIONS

The aggregation behavior of a surfactant-like IL, 1-butyl-3-methyl imidazolium octylsulfate, $[\text{C}_4\text{mim}][\text{C}_8\text{OSO}_3]$, is explored in the aqueous solutions of ethylene glycol (EG), ethylene glycol monomethyl ether (EGMME), or ethylene glycol dimethyl ether (EGDME). Various thermodynamic parameters show that both the increase in concentration of organic additive or EG derivatization decreases the spontaneity of aggregation. It is observed that, at low organic solvent concentration, ΔH_m° governs the change in ΔG_m° , while $-T\Delta S_m^\circ$ dictates the change at higher organic solvent concentration. The N_{agg} obtained from ^1H NMR spectroscopy decreases with the increase in content of EG/its derivatives, and for the same amount of EG/its derivatives, it follows the order $\text{H}_2\text{O} > \text{EG} > \text{EGMME} > \text{EGDME}$.

■ ASSOCIATED CONTENT

■ Supporting Information

Thermodynamic parameters are given as Table S1, emission spectra of pyrene is provided in Figure S1, and changes in NMR chemical shift for various cation and anion protons of IL in different systems are provided in Figures S2–S5, changes in NMR chemical shift for protons of EG derivatives are represented in Figures S6 and S7. This material is available free of charge via the Internet at <http://pubs.acs.org>.

■ AUTHOR INFORMATION

Corresponding Author

*E-mail: tejwant.tej@gmail.com (T.S.); mailme_arvind@yahoo.com, arvind@csmcri.org (A.K.). Phone: +91-278-2567039. Fax: +91-278-2567562.

Present Address

[†]Department of Chemistry and Biochemistry, Graduate School of Engineering, Kyushu University, Moto-oka-744, Nishi-ku, Fukuoka-819-0395, Japan.

■ ACKNOWLEDGMENTS

The authors are thankful to Department of Science and Technology (DST), Government of India, for financial support for this work (Nos. SR/S/PC-55/2008 and SR/S/PC-04/2010).

■ REFERENCES

- (1) *Ionic Liquids in Synthesis*; Wasserscheid, P., Welton, T., Eds.; Wiley: New York, 2003.
- (2) Earle, M. J.; McCormac, P. B.; Seddon, K. R. *Chem. Commun.* **1998**, 2245.
- (3) Welton, T. *Chem. Rev.* **1999**, 99, 2071.
- (4) Holbrey, J. D.; Seddon, K. R. *Clean Prod. Processes* **1999**, 1, 223.
- (5) Adams, C. J.; Earle, M. J.; Roberts, G.; Seddon, K. R. *Chem. Commun.* **1998**, 2097.
- (6) Leadbeater, N. E.; Torenus, H. M. *J. Org. Chem.* **2002**, 67, 3145.
- (7) Wasserscheid, P.; Keim, W. *Angew. Chem., Int. Ed.* **2000**, 39, 3772.
- (8) Anderson, J. L.; Ding, J.; Welton, T.; Armstrong, D. W. *J. Am. Chem. Soc.* **2002**, 124, 14247.
- (9) Rogers, R. D.; Seddon, K. R. *Science* **2003**, 302, 792.
- (10) Seddon, K. R. *Nat. Mater.* **2003**, 2, 363.
- (11) Earle, M. J.; Esperanca, J. M. S. S.; Gilea, M. A.; Canongia Lopes, J. N.; Rebelo, L. P. N.; Magee, J. W.; Seddon, K. R.; Widergren, J. A. *Nature* **2006**, 439, 831.
- (12) Santos, L. M. N. B. F.; Lopes, J. N. C.; Coutinho, J. A. P.; Esperanca, J. M. S. S.; Gomes, L. R.; Marrucho, I. M.; Rebelo, L. P. N. *Ionic Liquids. J. Am. Chem. Soc.* **2007**, 129, 284.
- (13) Bowers, J.; Butts, P.; Martin, J.; Vergara-Gutierrez, C.; Heenan, K. *Langmuir* **2004**, 20, 2191.
- (14) Miskolczy, Z.; Sebok-Nagy, K.; Biczok, L.; Goektuerk, S. *Chem. Phys. Lett.* **2004**, 400, 296.
- (15) Katayanagi, H.; Nishikawa, K.; Shimoza, H.; Miki, K.; Westh, P.; Koga, Y. *J. Phys. Chem. B* **2004**, 108, 19451.
- (16) Inoue, T.; Ebina, H.; Dong, B.; Zheng, L. Q. *J. Colloid Interface Sci.* **2007**, 314, 236.
- (17) Dong, B.; Gao, Y.; Su, Y.; Zheng, L.; Xu, J.; Inoue, T. *J. Phys. Chem. B* **2010**, 114, 340.
- (18) Dong, B.; Li, N.; Zheng, L.; Yu, L.; Inoue, T. *Langmuir* **2007**, 23, 4178.
- (19) Consorti, C. S.; Suarez, P. A. Z.; De Souza, R. F.; Burrow, R. A.; Farrar, D. H.; Lough, L. H.; Loh, W.; Da Silva, L. H. M.; Dupont, J. J. *J. Phys. Chem. B* **2005**, 109, 4341.
- (20) Zhao, Y.; Gao, S. J.; Wang, J. J.; Tang, J. M. *J. Phys. Chem. B* **2008**, 112, 2031.
- (21) Goodchild, I.; Collier, L.; Millar, S. L.; Prokes, I.; Lord, J. C. D.; Butts, C. P.; Bowers, J.; Webster, J. R.; Heenan, R. K. *J. Colloid Interface Sci.* **2007**, 307, 455.
- (22) Wang, J.; Wang, H.; Zhang, S.; Zhang, H.; Zhao, Y. *J. Phys. Chem. B* **2007**, 111, 6181.
- (23) Singh, T.; Kumar, A. *J. Phys. Chem. B* **2008**, 112, 4079.
- (24) Singh, T.; Drechsler, M.; Müller, A. H. E.; Mukhopadhyay, I.; Kumar, A. *Phys. Chem. Chem. Phys.* **2010**, 12, 11728.
- (25) Singh, T.; Kumar, A. *Colloids Surf., A* **2008**, 318, 263.
- (26) Blesic, M.; Marques, M. H.; Plechkova, N. V.; Seddon, K. R.; Rebelo, L. P. N.; Lopes, A. *Green Chem.* **2007**, 9, 481.
- (27) Blesic, M.; Lopes, A.; Melo, E.; Petrovski, Z.; Plechkova, N. V.; Canongia Lopes, J. N.; Seddon, K. R.; Rebelo, L. P. N. *J. Phys. Chem. B* **2008**, 112, 8645.
- (28) Smirnova, N. A.; Vanin, A. A.; Safonova, E. A.; Pukinsky, I. B.; Anufrikov, Y. A.; Makarov, A. L. *J. Colloid Interface Sci.* **2009**, 336, 793.
- (29) Luczak, J.; Jungnickel, C.; Joskowska, M.; Thöming, J.; Hupka, J. *J. Colloid Interface Sci.* **2009**, 336, 111.
- (30) Wang, H.; Wang, J.; Zhang, S.; Xuan, X. *J. Phys. Chem. B* **2008**, 112, 16682.
- (31) Thomaier, S.; Kunz, W. *J. Mol. Liq.* **2007**, 130, 104.
- (32) Li, N.; Zhang, S.; Zheng, L.; Dong, B.; Li, X.; Yu, L. *Phys. Chem. Chem. Phys.* **2008**, 10, 4375.
- (33) Bowlas, C. J.; Bruce, D. W.; Seddon, K. R. *Chem. Commun.* **1996**, 1625.
- (34) Gordon, C. M.; Holbrey, J. D.; Kennedy, A. R.; Seddon, K. R. *J. Mater. Chem.* **1998**, 8, 2627.
- (35) Adams, C. J.; Bradley, A. E.; Seddon, K. R. *Aust. J. Chem.* **2001**, 54, 679.
- (36) Zhou, Y.; Antonietti, M. *Chem. Mater.* **2004**, 16, 544.
- (37) Dattelbaum, A. M.; Baker, S. N.; Baker, G. A. *Chem. Commun.* **2005**, 939.
- (38) Wang, T.; Kaper, H.; Antonietti, M.; Smarsly, B. *Langmuir* **2007**, 23, 1489.
- (39) Domańska, U.; Pobudkowska, A.; Rogalski, M. *J. Colloid Interface Sci.* **2008**, 322, 342.
- (40) Zhang, G.; Chen, X.; Zhao, Y.; Xie, Y.; Qiu, H. *J. Phys. Chem. B* **2007**, 111, 11708.
- (41) Wang, J.; Zhang, L.; Wang, H.; Wu, C. *J. Phys. Chem. B* **2011**, 115, 4955.
- (42) Pino, V.; Yao, C.; Anderson, J. L. *J. Colloid Interface Sci.* **2009**, 333, 548.
- (43) Armstrong, D. W. *Sep. Purif. Methods* **1985**, 14, 213.
- (44) Thomas, D. P.; Foley, J. P. *J. Chromatogr., A* **2007**, 1149, 282.
- (45) Pan, S.; Liu, X.; Xie, Y.; Yi, Y.; Li, C.; Yan, Y.; Liu, Y. *Bioresour. Technol.* **2010**, 101, 9822.
- (46) Mizuuchi, H.; Jaitely, V.; Murdan, S.; Florence, A. T. *Eur. J. Pharm. Sci.* **2008**, 33, 326.
- (47) Zuo, Y.; Chen, J.; Li, D. *Sep. Purif. Technol.* **2008**, 63, 77.
- (48) Prasad, M.; Moulik, S. P.; Chisholm, D.; Palepu, R. *J. Oleo Sci.* **2003**, 52, 523.
- (49) Lindman, B.; Söderman, O.; Wennerström, H. In *Surfactant Solutions: New Methods of Investigation*; Zana, R., Ed.; Marcel Dekker: New York, 1987; Chapter 6.
- (50) Leibfritz, D.; Roberts, J. D. *J. Am. Chem. Soc.* **1973**, 95, 4996.
- (51) Drakenberg, T.; Lindman, B. *J. Colloid Interface Sci.* **1973**, 44, 184.
- (52) Ruso, J. M.; Attwood, D.; Taboada, P.; Mosquera, V.; Sarmiento, F. *Langmuir* **2000**, 16, 1620.
- (53) Luchetti, L.; Mancini, G. *Langmuir* **2000**, 16, 161.
- (54) Hassan, P. A.; Srinivasa R. Raghavan, S. R.; Kaler, E. W. *Langmuir* **2002**, 18, 2543.
- (55) Shimizu, S.; Pires, P. A. R.; Fish, H.; Halstead, T. K.; Seoud, O. W. A. *Phys. Chem. Chem. Phys.* **2003**, 5, 3489.
- (56) Flodström, K.; Wennerström, H.; Alfredsson, V. *Langmuir* **2004**, 20, 680.
- (57) Nardsterna, L.; Furö, I.; Stilbs, P. *J. Am. Chem. Soc.* **2006**, 128, 6704.
- (58) Singh, T.; Kumar, A. *J. Phys. Chem. B* **2008**, 112, 4079.

- (59) Saxena, A.; Antony, T.; Bohidar, H. B. *J. Phys. Chem. B* **1998**, *102*, 5063.
- (60) Carpena, P.; Aguiar, J.; Bernaola-Galván, P.; Carnero Ruiz, C. *Langmuir* **2002**, *18*, 6054.
- (61) Phillips, J. N. *Trans. Faraday Soc.* **1955**, *51*, 561.
- (62) Bakshi, M. S.; Kaur, I. *Colloid Polym. Sci.* **2003**, *281*, 935.
- (63) Nagarajan, R.; Wang, C. C. *J. Colloid Interface Sci.* **1996**, *178*, 471.
- (64) Nagarajan, R.; Wang, C. C. *Langmuir* **2000**, *16*, 5242.
- (65) Marcus, Y. *Ion Solvation*; Wiley: London, 1986.
- (66) Rodríguez, A.; Graciani, M. M.; Fernández, G.; Moyá, M. L. *J. Colloid Interface Sci.* **2009**, *338*, 207.
- (67) Ramadan, M.; Evans, D. F.; Lumry, R.; Philson, S. *J. Phys. Chem.* **1985**, *89*, 3405.
- (68) Rodríguez, A.; Graciani, M. M.; Moyá, M. L. *Langmuir* **2008**, *24*, 12785.
- (69) Jaycock, M. J.; Parfitt, G. D. *Chemistry of Interfaces*; John Wiley and Sons: New York, 1981.
- (70) Kalyanasundaram, K.; Thomas, J. K. *J. Am. Chem. Soc.* **1977**, *99*, 2039.
- (71) Alonso, B.; Harris, R. K.; Kenwright, A. M. *J. Colloid Interface Sci.* **2002**, *251*, 366.
- (72) Tonelli, A. E. *NMR spectroscopy and polymer microstructure: the conformational connection*; VCH: New York, 1989.
- (73) Persson, B. -O.; Darkenberg, T.; Lindman, B. *J. Phys. Chem.* **1976**, *80*, 2124.
- (74) Persson, B. -O.; Darkenberg, T.; Lindman, B. *J. Phys. Chem.* **1979**, *83*, 3011.